RESEARCH REPORT

Acetylcholinesterase plays a non-neuronal, non-esterase role in organogenesis

Melissa A. Pickett[1], Michael K. Dush[2] and Nanette M. Nascone-Yoder[1,2,*]

ABSTRACT

Acetylcholinesterase (AChE) is crucial for degrading acetylcholine at cholinergic synapses. *In vitro* studies suggest that, in addition to its role in nervous system signaling, AChE can also modulate non-neuronal cell properties, although it remains controversial whether AChE functions in this capacity *in vivo*. Here, we show that AChE plays an essential non-classical role in vertebrate gut morphogenesis. Exposure of *Xenopus* embryos to AChE-inhibiting chemicals results in severe defects in intestinal development. Tissue-targeted loss-of-function assays (via microinjection of antisense morpholino or CRISPR-Cas9) confirm that AChE is specifically required in the gut endoderm tissue, a non-neuronal cell population, where it mediates adhesion to fibronectin and regulates cell rearrangement events that drive gut lengthening and digestive epithelial morphogenesis. Notably, the classical esterase activity of AChE is dispensable for this activity. As AChE is deeply conserved, widely expressed outside of the nervous system, and the target of many environmental chemicals, these results have wide-reaching implications for development and toxicology.

KEY WORDS: Acetylcholinesterase, Morphogenesis, Gut, Intestine, Fibronectin, *Xenopus laevis*

INTRODUCTION

Acetylcholinesterase (AChE) is a highly conserved protein extensively studied for its essential enzymatic role in degrading the neurotransmitter acetylcholine at neural synapses (Silman and Sussman, 2005; Soreq and Seidman, 2001). This esterase activity is the target of widely used pesticides and pharmaceuticals (Mileson et al., 1998; Pope et al., 2005), yet the broad expression of AChE outside of the nervous system (Anderson et al., 2008; Bertrand et al., 2001; Bicker et al., 2004; Drews, 1975) and similarity to adhesion molecules (Botti et al., 1998; Darboux et al., 1996) suggest that it has additional functions. Indeed, in neuronal and non-neuronal cell lines, AChE promotes cell-substrate adhesion (Inkson et al., 2004; Johnson and Moore, 1999; Sharma et al., 2001; Syed et al., 2008), polarized cell migration (Anderson et al., 2008), cytoskeletal organization (Dupree and Bigbee, 1994; Keller et al., 2001) and cell differentiation (Grisaru et al., 1999; Xiang et al., 2008), independently of its esterase activity (Layer et al., 1993). However, the *in vivo* relevance of this putative multi-functionality is poorly substantiated, especially in non-neuronal contexts (Vogel-Hopker et al., 2012).

[1]Department of Biology, Environmental and Molecular Toxicology Program, North Carolina State University, Raleigh, NC 27606, USA. [2]Department of Molecular Biomedical Sciences, College of Veterinary Medicine, North Carolina State University, Raleigh, NC 27607, USA.

*Author for correspondence (nmnascon@ncsu.edu)

N.M.N., 0000-0003-1301-5298

In the embryo, AChE is expressed in both neuronal and non-neuronal cell populations undergoing cell migration, rearrangement, and differentiation (Bicker et al., 2004; Drews, 1975; Ohta et al., 2009). Consistent with this expression, embryo exposure to chemical inhibitors of AChE is associated with structural defects not only in the nervous system, but also in the heart and digestive tract of vertebrates (Pamanji et al., 2015a,b; Snawder and Chambers, 1989; Wyttenbach and Thompson, 1985), including humans (Carmichael et al., 2014; Romero et al., 1989; Sherman, 1995). Although such teratogenicity implicates AChE in non-neuronal organogenesis, genetic evidence is inconclusive. AChE null mutants have severe behavioral and neural patterning deficits, consistent with its classical functions, but appear otherwise normal (Behra et al., 2002; Bytyqi et al., 2004; Downes and Granato, 2004; Duysen et al., 2002; Xie et al., 2000). This has prompted speculation that non-neuronal defects observed following exposure to chemical AChE inhibitors reflect off-target effects (Behra et al., 2004) or that *in vitro* morphogenetic functions of AChE are irrelevant/redundant *in vivo* (Cousin et al., 2005; Johnson et al., 2008b). Nonetheless, recent studies report a non-neural function of AChE during skeletogenesis in both mouse and chick (Spieker et al., 2016, 2017), indicating that phenotypic differences due to non-classical AChE functions might have been missed in earlier studies. Additionally, *Ache*^{−/−} mice exhibit developmental delay and suffer a fatal growth/nutritional deficiency with unknown etiology (Duysen et al., 2002; Xie et al., 2000). Likewise, *ache* null zebrafish larvae die with severe edema, a condition that can result from abnormal morphogenesis in several organs (Behra et al., 2002; Downes and Granato, 2004). To date, non-neuronal organogenesis has not been examined at the cellular level in AChE-deficient contexts, and the significance of AChE outside of the nervous system remains equivocal.

RESULTS AND DISCUSSION
AChE is required for gut morphogenesis

Associations between AChE inhibitor exposure and digestive tract anomalies (Aronzon et al., 2014; Bacchetta et al., 2008; Snawder and Chambers, 1989) suggest that AChE might play a role in gut development. However, exposures in these studies were continuous from the embryonic blastula stage, and cannot exclude the possibility that early actions of the chemicals were manifested later as secondary intestinal malformations. To determine whether AChE is specifically required for intestinal development, *Xenopus laevis* frog embryos were exposed to AChE inhibitors only during gut morphogenesis [NF 33-46 (Nieuwkoop and Faber, 1994)] at tailbud stages, well after the completion of early germ layer specification and patterning events. Exposure to organophosphate pesticides (malathion or chlorpyrifos-methyl) during this developmental window resulted in short, malrotated intestines compared with DMSO-treated control siblings (Fig. 1A-C′,E). Identical results were elicited by exposure to the structurally unrelated Alzheimer's drug Huperzine A (Ashani et al.,

DEVELOPMENT
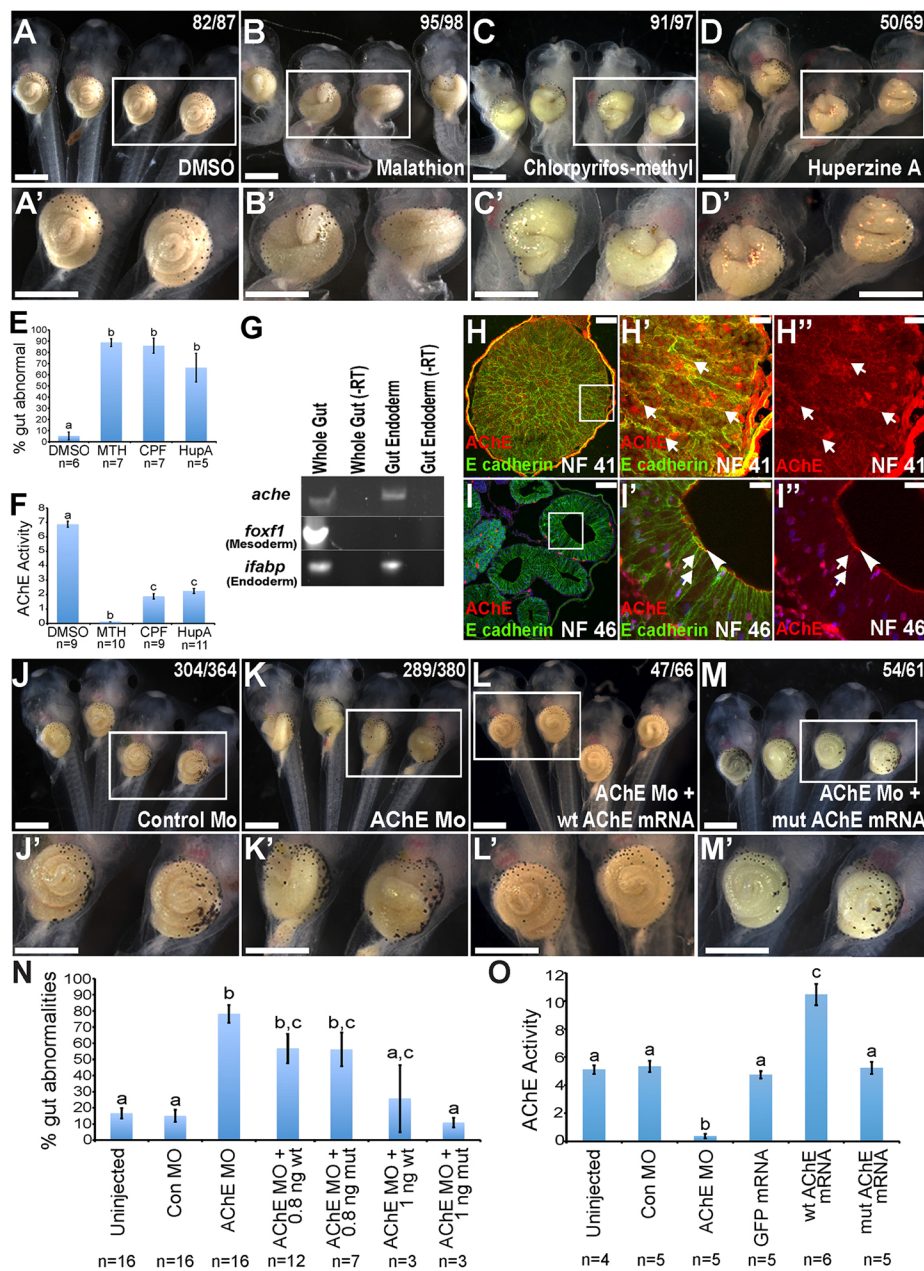
Fig. 1. AChE plays a non-neuronal, non-esterase role in intestine organogenesis. Normal intestinal elongation and rotation are observed in DMSO-exposed control tadpoles (A,A′). Exposure to malathion (MTH; B,B′), chlorpyrifos-methyl (CPF; C,C′) or Huperzine A (HupA; D,D′) increases the percentage (E) of tadpoles with short/malrotated intestines. AChE activity assays (F) confirm that the applied compounds inhibit AChE *in vivo*. RT-PCR (G) indicates that isolated intestinal endoderm (indicated by the expression of *ifabp*, but not *foxf1*) expresses *ache*. −RT, control lacking reverse transcriptase. At NF 41, AChE (red) colocalizes with E-cadherin (green) at endoderm cell membranes (H-H″, arrows). By NF 46, AChE is apically enriched (I-I″, arrowheads), with reduced lateral membrane expression (arrows). Intestinal development is normal in control MO-injected embryos (J,J′,N), whereas microinjection of AChE MO results in short/malrotated intestines (K,K′,N). Intestinal malformations are rescued by co-injection of RNA encoding wt AChE (L,L′,N) or mutAChE that lacks catalytic activity (M,M′,N). AChE activity assays (O) confirm that AChE MO knocks down AChE, that wt AChE mRNA increases activity, and that mutAChE mRNA has no effect on AChE activity, relative to controls (uninjected, control MO, *GFP* mRNA). Higher magnification views of the boxed regions in A-D,H-M are shown in A′-D′, H′-M′, respectively. The number of tadpoles with the phenotype shown among the total number of tadpoles in that experimental group is indicated (A-D,J-M). Bar charts show mean±s.e.m. Significant differences between the percentage of tadpoles with abnormal gut phenotypes or between AChE activities from *n*=3-16 independent experiments (16-30 embryos per condition per experiment) are indicated by lowercase letters (*P*<0.05). Scale bars: 1000 μm in A-D′,J-M′; 100 μm in H,I; 25 μm in H′-I″.

1992) (Fig. 1D-E), suggesting that gut phenotypes result from inhibition of AChE activity (Fig. 1F), as opposed to organophosphate-related off-target effects.

During *Xenopus* gut development, *ache* is expressed in the endoderm cells (Fig. 1G) that rearrange to lengthen the intestine and form the digestive epithelium (Reed et al., 2009). During gut elongation, AChE is localized to endoderm cell membranes (Fig. 1H-I′). This expression is consistent with previous reports of AChE activity within the developing gut of chick and amphibian embryos (Drews, 1975) and suggests that AChE might play conserved, non-neuronal role(s) in intestinal organogenesis. AChE becomes localized to the apical surface by NF 46 (Fig. 1I-I″), consistent with a potential function in cell polarity (Anderson et al., 2008).

To confirm that AChE is required for intestinal morphogenesis, we microinjected morpholino oligonucleotide (MO) to knock down translation of AChE protein in the embryo. Unfortunately, embryos injected with AChE MO at the 1-cell stage (ubiquitous knockdown)

die prior to morphogenesis of the intestine, consistent with similar results in zebrafish (Behra et al., 2002; Downes and Granato, 2004). To overcome this limitation, we performed targeted microinjection at the 8-cell stage to specifically knock down AChE in intestinal endoderm (Reed et al., 2009). As with chemical inhibition of AChE, endoderm-limited AChE knockdown results in short, malrotated guts compared with control MO-injected siblings (Fig. 1J-K′,N), indicating that AChE protein is required specifically within this non-neuronal tissue for intestinal morphogenesis.

Importantly, co-injection of AChE MO with a MO-resistant wild-type (wt) *ache* mRNA (wt AChE; supplementary Materials and Methods) rescues gut defects, confirming that morphant phenotypes result specifically from AChE knockdown (Fig. 1L,L′,N). Efficacy of the AChE MO and wt AChE mRNA were confirmed by immunostaining for AChE in injected regions of the gut tube: AChE MO results in loss of AChE protein from the apical surface of injected cells, and expression is restored by co-injection of wt AChE

(Fig. S1). Additionally, enzymatic activity assays performed with embryos injected with AChE MO or wt AChE mRNA show that the reagents have the expected impact on AChE esterase function (Fig. 1O). Finally, embryos with CRISPR-Cas9-generated *ache* mutations also exhibit disrupted intestinal development (Fig. S2), further confirming a requirement for AChE in gut morphogenesis.

Non-esterase functions of AChE are required for gut morphogenesis

Blocking the esterase activity of AChE is neurotoxic because it leads to excessive cholinergic signaling via acetylcholine receptors (AChR). Therefore, if the gut defects that result from AChE deficiency are caused by excessive cholinergic signaling, gut malformations should also be induced by exposure to AChR agonists (e.g. carbachol). Likewise, co-exposure to AChR antagonists, which block cholinergic signaling (e.g. atropine), should rescue any gut defects elicited by AChE inhibitors. Surprisingly, neither carbachol nor atropine exposure affects gut development in the presence or absence of AChE inhibitors, although exposure to these compounds has predictable effects on embryonic lethality, confirming the activity of these chemicals (Fig. S3). This suggests that the esterase activity of AChE is dispensable for gut morphogenesis.

To further investigate non-esterase function(s), we generated a mutated *ache* mRNA (mutAChE; supplementary Materials and Methods) that lacks catalytic activity when translated. Although mutAChE has no effect on endogenous AChE esterase activity levels (Fig. 1O), co-injection of mutAChE with AChE MO nonetheless rescued intestinal development to the same extent as wt AChE mRNA (Fig. 1M-N), and restored AChE localization in the intestinal epithelium (Fig. S1). These results suggest that AChE has essential non-esterase functions *in vivo* during gut morphogenesis.

AChE is required for endoderm rearrangement and epithelialization

Although AChE can influence rates of cell proliferation and apoptosis in other contexts (Anderson et al., 2008; Grisaru et al., 1999; Yang

et al., 2002), these parameters are unaffected in AChE MO-injected guts (data not shown), suggesting that AChE regulates gut morphogenesis without affecting cell number. During the formation of the *Xenopus* intestine, endoderm cells radially intercalate, driving gut tube elongation as concentric cell layers are reduced from four or five cells thick to a single layer (Chalmers and Slack, 2000; Reed et al., 2009). In this process, endoderm cells polarize, change shape, reorganize their cytoskeletal architecture, and differentiate into a mature epithelium (Dush and Nascone-Yoder, 2013; Reed et al., 2009). We investigated whether AChE regulates these events.

In control MO-injected embryos, the loops of elongated intestine (NF 46) are lined by a single layer of endoderm-derived columnar epithelium (Figs 2 and 3), which exhibits apical localization of aPKC (Fig. 2A,E,I). Parallel arrays of microtubules are oriented along the apicobasal axis and enriched apically (Fig. 3A,E,I). Robust expression of IFABP (FABP2), a marker of intestinal fate in the small intestine (Chalmers and Slack, 1998), indicates that control MO-injected endoderm cells differentiate into functional digestive epithelium (Fig. 3M,Q).

By contrast, multiple cell layers are present in the intestinal epithelium of AChE MO-injected embryos, indicative of defective endoderm rearrangement (Fig. 2B,F,J). The AChE MO-injected cells are rounder in shape (Fig. 2J, Fig. S4) and fail to form a polarized epithelium, as revealed by the absence of aPKC in injected cells (Fig. 2B,F,J). Endoderm cells lacking AChE also display disorganized microtubules that do not align with any cell axis and show no evidence of apical enrichment (Fig. 3B,F,J). Finally, expected markers of intestinal differentiation (IFABP) are absent in AChE MO-injected cells (Fig. 3N,R).

Importantly, the extensive cellular defects elicited by AChE MO are rescued by co-injection of either wt AChE mRNA (Fig. 2C,G,K, Fig. 3C,G,K,O,S, Fig. S4) or the catalytically inactive mutAChE (Fig. 2D,H,L, Fig. 3D,H,L,P,T, Fig. S4), demonstrating that AChE directs cellular events *in vivo* via a non-esterase mechanism. Exposure to AChE-inhibiting chemicals results in similar defects in
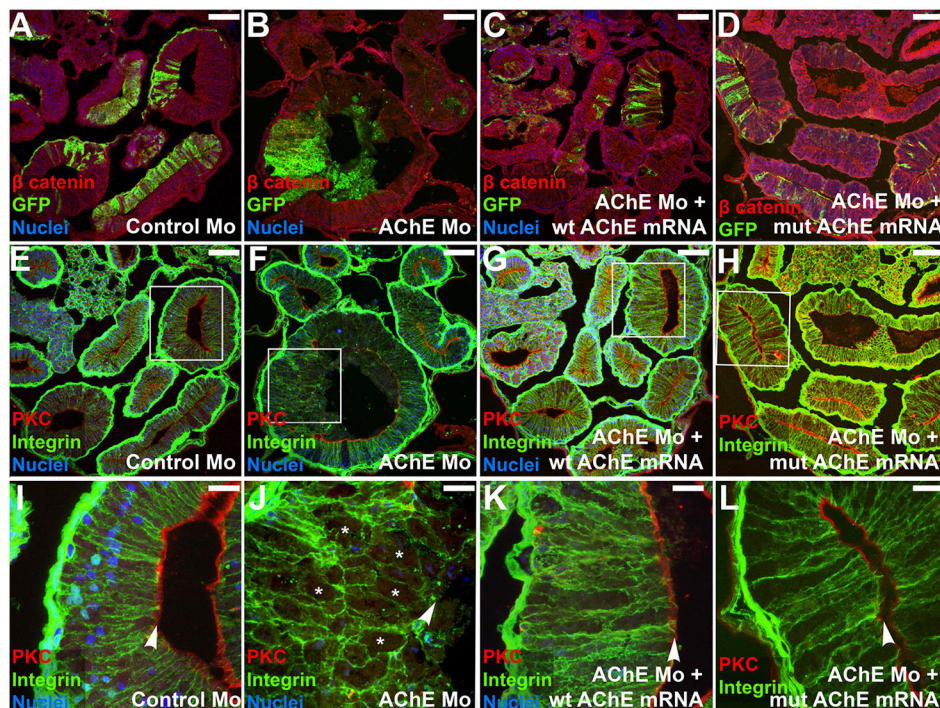

Fig. 2. AChE is required for endoderm cell rearrangement and polarization. In NF 46 intestine sections of embryos injected with control MO (A), AChE MO (B), AChE MO plus wt AChE mRNA (C), or AChE MO plus mutAChE mRNA (D), β-catenin (red) outlines membranes of injected (GFP labeled, green) and uninjected cells. Serial sections from embryos in A-D were immunostained for integrin (green) and aPKC (red) (E-H); the boxed regions are shown at higher magnification in I-L. A single-layer columnar epithelium of polarized cells forms in control MO-injected intestines (I). AChE MO-injected cells (J) are rounder (asterisks), unpolarized [absence of aPKC (red), arrowhead] and fail to form a single layer. Defects are rescued by co-injection with wt AChE mRNA (K) or mutAChE mRNA (L). Scale bars: 100 µm in A-H; 25 µm in I-L.
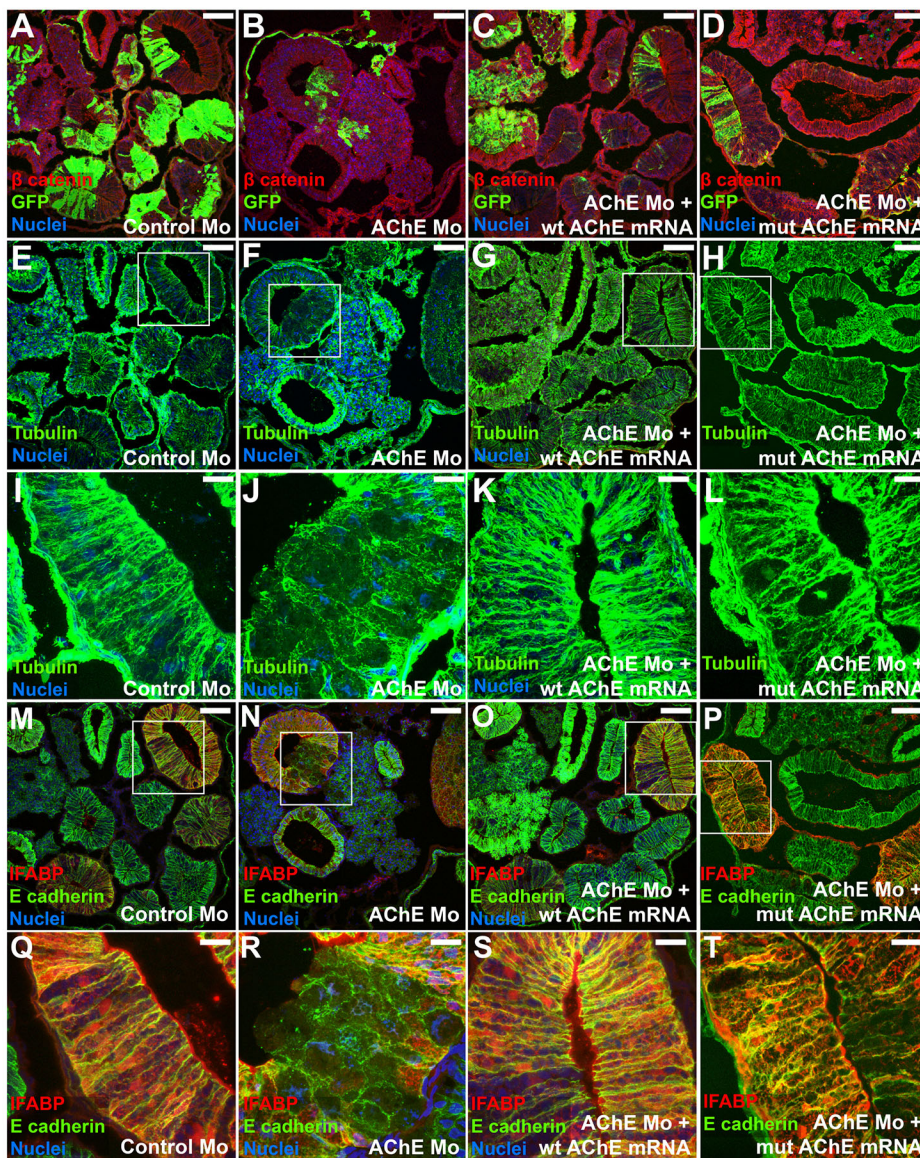
Fig. 3. AChE is required for microtubule organization and endoderm differentiation. In NF 46 intestine sections of embryos injected with control MO (A), AChE MO (B), AChE MO plus wt AChE mRNA (C), or AChE MO plus mutAChE mRNA (D), β-catenin (red) outlines cell membranes of injected (GFP labeled, green) and uninjected cells. Serial sections from embryos in A-D were immunostained to visualize microtubules (α-tubulin, green) (E-H); boxed regions are shown at higher magnification in I-L. Microtubules are apically enriched and oriented along the apical-basal axis of columnar epithelial cells (I). Microtubule organization is disrupted when AChE is knocked down (J), but is rescued by co-injection of the AChE MO with wt AChE mRNA (K) or mutAChE mRNA (L). Serial sections from embryos in A-H were immunostained for E-cadherin (green) and IFABP (red) (M-P); boxed regions are shown at higher magnification in Q-T. IFABP is expressed in control MO-injected intestine (Q). AChE knockdown (R) prevents differentiation of the endoderm, as indicated by the absence of IFABP in AChE MO-injected cells. Differentiation is restored by co-injection of the AChE MO with wt AChE mRNA (S) or mutAChE mRNA (T). Nuclei, blue (TO-PRO-3). Scale bars: 100 μm in A-H,M-P; 25 μm in I-L,Q-T.

endoderm cell shape and polarity (Fig. S5), suggesting environmental exposure to such compounds not only perturbs cholinergic signaling, but can also disrupt esterase-independent morphogenetic functions of AChE in non-neuronal tissues.

AChE is not required for endoderm cell-cell adhesion
AChE shares homology with catalytically inactive cholinesterase-like adhesion molecules (Gilbert and Auld, 2005). Changes in endoderm cell-cell adhesion are linked to abnormal intestine morphogenesis (Dush and Nascone-Yoder, 2013; Reed et al., 2009). To determine if AChE is required for gut endoderm cell-cell adhesion, we employed an *ex vivo* dissociation/reaggregation assay (supplementary Materials and Methods) (Dush and Nascone-Yoder, 2013). In this assay, dissociated single-cell suspensions of AChE MO-injected endoderm cells were able to reaggregate to the same degree as uninjected or control MO-injected cells, indicating that AChE is not required for cell-cell adhesion (Fig. 4A,B). Furthermore, neither *in vivo* nor *ex vivo* exposure to AChE-inhibiting chemicals, AChR agonists or AChR antagonists affected reaggregation (Fig. S6), suggesting AChE activity is unnecessary for intercellular adhesion in the gut.

AChE is required for endoderm adhesion to fibronectin
In vitro, AChE binds to extracellular matrix (ECM) ligands, promoting cell-substrate adhesion (Johnson and Moore, 1999, 2004; Johnson et al., 2008a). Laminin (LM) and fibronectin (FN) are among the ECM proteins required for intestinal development (Davidson et al., 2006; Kedinger et al., 1998; Marsden and DeSimone, 2001; Yarnitzky and Volk, 1995). LM is localized to the basement membrane (BM) (Fig. 4C,C′), and plays a role in BM assembly and differentiation of the digestive epithelium (Kedinger et al., 1998; Yarnitzky and Volk, 1995). FN is likewise found at the BM but is additionally enriched at apicobasal poles of intercalating endoderm cells (Fig. 4D,D′). Like AChE-deficient guts, FN-deficient guts are severely shortened (Davidson et al., 2006; Marsden and DeSimone, 2001).

To determine if AChE is required for endoderm-ECM adhesion, endoderm cells from control MO- or AChE MO-injected guts were dissociated into a single-cell suspension and plated on LM or FN substrates (supplementary Materials and Methods). Although AChE-LM interactions are well described in other contexts (Johnson et al., 2008a; Paraoanu and Layer, 2004), we found that intestinal endoderm adhesion on LM was independent of AChE (Fig. 4E). Other studies have similarly failed to identify AChE-
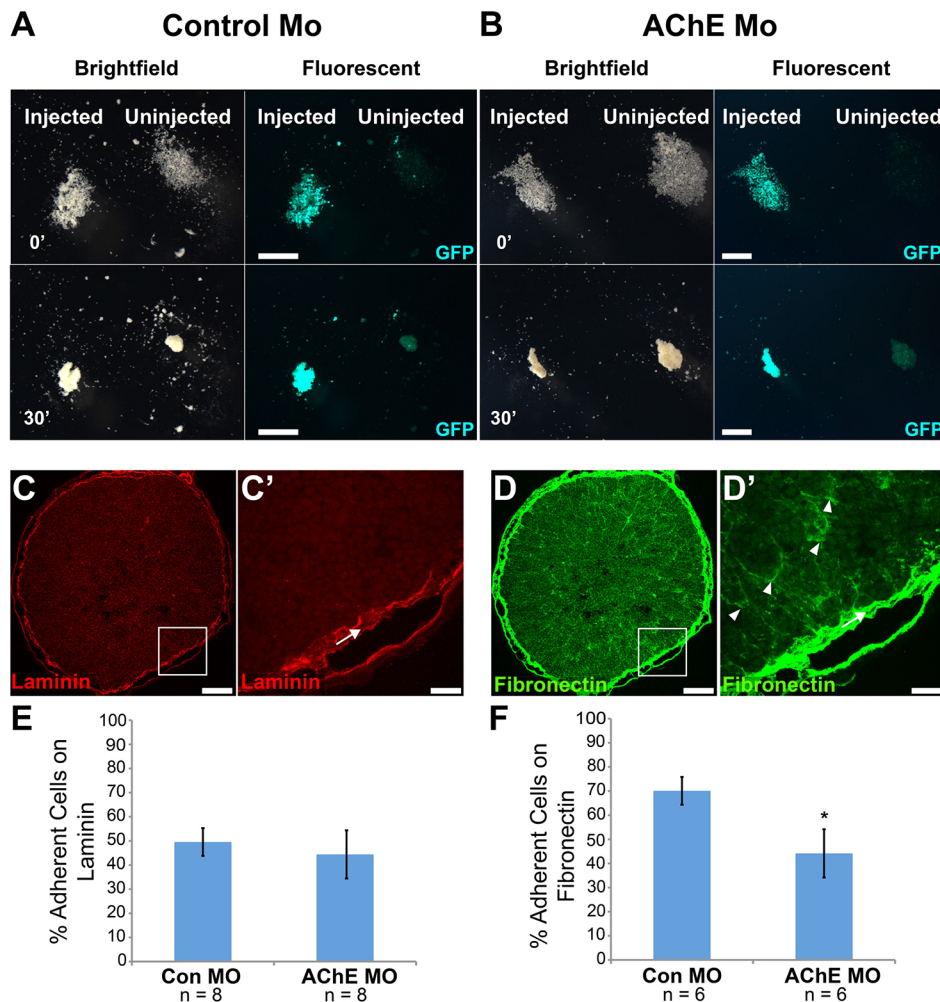
Fig. 4. AChE is not required for cell-cell adhesion, but is necessary for cell-substrate adhesion to fibronectin.
Dissociated intestinal endoderm cells from control MO-injected (A) or AChE MO-injected (B) embryos reaggregated 30 min (30′) after introduction of Ca^{2+} ions into the medium (0′; see supplementary Materials and Methods). Brightfield/fluorescent images show that both injected and uninjected cells from each injection group reaggregated. Assays were performed using at least three different embryos per condition. Transverse sections through wild-type guts (NF 41) were immunostained for laminin (LM; C,C′) or fibronectin (FN; D,D′). LM (red) is found at basement membranes (arrow) surrounding the gut tube. FN (green) is found at the basement membrane (arrow), but is also enriched at endoderm cell basal poles (arrowheads). Endoderm cells from control MO-injected or AChE MO-injected intestines were plated on LM (E) or FN (F). There is no difference in cell adhesion on LM (E), but cells from AChE MO-injected embryos are less adherent than control cells on FN (F). Mean±s.e.m. for the percentage of adherent cells for six to eight independent embryos. *$P<0.05$. Scale bars: 1000 μm in A,B; 100 μm in C,D; 25 μm in C′,D′.

dependent adhesion on LM (Anderson et al., 2008; Sharma et al., 2001), suggesting this interaction is cell type-specific. However, we did find that AChE MO-injected endoderm cells were significantly less adherent on FN compared with control MO-injected cells (Fig. 4F). These results are consistent with AChE-dependent adhesion of colon cancer cells on FN, but not LM, substrates (Syed et al., 2008), and suggest that AChE promotes gut morphogenesis via an FN-dependent mechanism.

Conclusions
Taken together, this study provides direct *in vivo* evidence for a morphogenetic function of AChE in non-neuronal embryonic tissues. AChE modulates key cell behaviors within the gut endoderm, a tissue that undergoes dramatic rearrangements to drive intestine lengthening and epithelialization (Cervantes et al., 2009; Dush and Nascone-Yoder, 2013; Matsuyama et al., 2009; Reed et al., 2009). As anomalous morphogenesis of the digestive epithelium could underlie nutrient malabsorption, our findings are consistent with the growth deficiency observed in $Ache^{-/-}$ mice (Duysen et al., 2002). Moreover, our results suggest that chemicals used to inhibit AChE esterase function (e.g. organophosphates) also perturb its *in vivo* morphogenetic activity; therefore, environmental exposure to such compounds may be an unrecognized risk factor for intestinal malformations (Carmichael et al., 2016).

AChE regulates gut development in a manner independent of its well-known esterase activity. The mechanism involves adhesion to FN, a molecule that modulates cell polarization and rearrangements

in many developmental contexts (Davidson et al., 2006; Marsden and DeSimone, 2003; Trinh and Stainier, 2004; Weber et al., 2012). As FN is distributed in a radially polarized manner within the gut tube, AChE-FN interactions are likely to facilitate endoderm cell polarization, orienting the radial rearrangements that are crucial to drive intestinal elongation. Moreover, the broad expression of AChE and FN during metazoan development, wound healing and regeneration (Anderson et al., 2008; Bertrand et al., 2001; Bicker et al., 2004; de Almeida et al., 2016; Drews, 1975; Ohta et al., 2009) suggests that AChE could regulate a wide variety of morphogenetic events across numerous species.

MATERIALS AND METHODS
Embryo culture
Xenopus laevis tadpoles were obtained by *in vitro* fertilization, in compliance with ethical regulations approved by North Carolina State University IACUC, staged, and anesthetized as described (Dush and Nascone-Yoder, 2013).

Chemical exposures
Embryos were exposed to AChE inhibitors (20 mg/l malathion, 5 mg/l chlorpyrifos-methyl, or 10 μM Huperzine A) or an equivalent volume of DMSO from NF 33 to NF 41-46 (Nieuwkoop and Faber, 1994). See the supplementary Materials and Methods for details.

AChE loss-of-function (MO and CRISPR) and mRNA rescue
MOs (GeneTools) were designed to bind to the 5′ UTR near the translation start site of *Xenopus laevis ache* mRNA (AChE MO,

5′-CATGGCTGCTCCTCTGTGGGATTAC-3′) or to human β-globin mRNA, a standard control (control MO, 5′-CCTCTTACCTCAGTTAC-AATTTATA-3′).

To achieve ubiquitous knockdown of AChE, embryos were injected at the 1-cell stage (40 ng). To target the intestinal endoderm, MOs were injected into a specific vegetal blastomere of the 8-cell embryo (7.6 ng), with *GFP* mRNA co-injected as a lineage tracer, as described (Reed et al., 2009). In rescue experiments, MO-resistant wt AChE or mutAChE mRNAs (800-1000 pg/blastomere) were co-injected with *GFP* mRNA. See the supplementary Materials and Methods for details of mRNA generation and synthesis.

For CRISPR-Cas9 experiments, *ache* gRNA was co-injected with Cas9 mRNA/protein [synthesized as described (Guo et al., 2014)] into 1- or 8-cell embryos (similar results were obtained with both injections). The *ache* gRNA target site was 5′-GGCAATCTTCACTCATTGGC-3′. For mutation analyses, genomic DNA from ten embryos injected with Cas9 plus *ache* gRNA was pooled and the genomic locus targeted by *ache* gRNA was PCR amplified using primers: F, 5′-ATGGCACTTGTACCCTTTGCTCAGCT-G-3′; and R, 5′-ATGTGGAACCCCCATCCACTGTGGCC-3′. PCR products were subcloned into pCRII vector (ThermoFisher Scientific) and individual clones were sequenced with M13R primer (5′-CAGGAAACA-GCTATGAC-3′) to determine mutation frequency.

AChE activity assays

AChE activity was determined as previously described (Bonfanti et al., 2004; Ellman et al., 1961) from at least five independent pools of four animals subject to (1) chemical exposure and harvested at NF 46 (see above) or (2) injected with MOs or wt AChE/mutAChE mRNAs (1200 pg) at the 1-cell stage (see above) and harvested at NF 35. See the supplementary Materials and Methods for details of the AChE activity assays.

Immunohistochemistry

Immunostaining was performed on transverse intestinal sections as described (Dush and Nascone-Yoder, 2013). Antibodies are listed in Table S1. Fluorescence was visualized on a Leica SPEII confocal microscope.

Ex vivo cell assays

Intestines were dissected from MO-injected NF 41-42 tadpoles and the gut endoderm cells dissociated as described (Dush and Nascone-Yoder, 2013). To examine cell-cell adhesion, injected and uninjected cells were separated by fluorescence and reaggregation assessed 30 min after reintroduction of Ca^{2+}/Mg^{2+} to the medium (MBS) (Sive et al., 2000). For cell-substrate adhesion, dissociated cells were applied to plastic plates coated with 50 µg/ml LM or FN and allowed to adhere for 60 min before washing and fixation. See the supplementary Materials and Methods for details.

Statistics

Analysis of variance (ANOVA) was used to evaluate differences in the mean percentage of gut phenotypes for chemical treatments ($n \geq 5$) and microinjection studies ($n \geq 3$), as well as AChE activity for chemical treatment ($n \geq 9$) and microinjections ($n \geq 4$), where n is the number of independent experiments performed with 16-30 grossly normal embryos (a generally accepted number of biological replicates) randomly distributed among each control or experimental condition. Experiments were excluded from analysis if abnormalities in control groups exceeded 25% of the population. Student's *t*-test was used to evaluate difference in means (in length:width) for injected and uninjected cells for each microinjection ($n \geq 3$), and for cell adhesion on LM ($n = 8$) and FN ($n = 6$). Differences were considered significant if $P \leq 0.05$. StatCrunch statistical software (Pearson) was used for analyses. Error bars in all graphs represent s.e.m.

Competing interests
The authors declare no competing or financial interests.

Author contributions
Conceptualization: M.A.P., N.M.N.-Y.; Methodology: M.A.P.; Validation: M.K.D.; Formal analysis: M.A.P.; Investigation: M.A.P., M.K.D.; Resources: N.M.N.-Y.; Writing - original draft: M.A.P., N.M.N.-Y.; Writing - review & editing: M.A.P., M.K.D., N.M.N.-Y.; Visualization: M.A.P.; Supervision: N.M.N.-Y.; Project administration: N.M.N.-Y.; Funding acquisition: N.M.N.-Y.

Supplementary information
Supplementary information available online at
http://dev.biologists.org/lookup/doi/10.1242/dev.149831.supplemental

References

Anderson, A. A., Ushakov, D. S., Ferenczi, M. A., Mori, R., Martin, P. and Saffell, J. L. (2008). Morphoregulation by acetylcholinesterase in fibroblasts and astrocytes. *J. Cell. Physiol.* **215**, 82-100.

Aronzon, C. M., Marino, D. J. G., Ronco, A. E. and Pérez Coll, C. S. (2014). Differential toxicity and uptake of Diazinon on embryo-larval development of *Rhinella arenarum*. *Chemosphere* **100**, 50-56.

Ashani, Y., Peggins, J. O., III and Doctor, B. P. (1992). Mechanism of inhibition of cholinesterases by huperzine A. *Biochem. Biophys. Res. Commun.* **184**, 719-726.

Bacchetta, R., Mantecca, P., Andrioletti, M., Vismara, C. and Vailati, G. (2008). Axial-skeletal defects caused by Carbaryl in *Xenopus laevis* embryos. *Sci. Total Environ.* **392**, 110-118.

Behra, M., Cousin, X., Bertrand, C., Vonesch, J.-L., Biellmann, D., Chatonnet, A. and Strahle, U. (2002). Acetylcholinesterase is required for neuronal and muscular development in the zebrafish embryo. *Nat. Neurosci.* **5**, 111-118.

Behra, M., Etard, C., Cousin, X. and Strähle, U. (2004). The use of zebrafish mutants to identify secondary target effects of acetylcholine esterase inhibitors. *Toxicol. Sci.* **77**, 325-333.

Bertrand, C., Chatonnet, A., Takke, C., Yan, Y. L., Postlethwait, J., Toutant, J.-P. and Cousin, X. (2001). Zebrafish acetylcholinesterase is encoded by a single gene localized on linkage group 7. *J. Biol. Chem.* **276**, 464-474.

Bicker, G., Naujock, M. and Haase, A. (2004). Cellular expression patterns of acetylcholinesterase activity during grasshopper development. *Cell Tissue Res.* **317**, 207-220.

Bonfanti, P., Colombo, A., Orsi, F., Nizzetto, I., Andrioletti, M., Bacchetta, R., Mantecca, P., Fascio, U., Vailati, G. and Vismara, C. (2004). Comparative teratogenicity of chlorpyrifos and malathion on *Xenopus laevis* development. *Aquat. Toxicol.* **70**, 189-200.

Botti, S. A., Felder, C. E., Sussman, J. L. and Silman, I. (1998). Electrotactins: a class of adhesion proteins with conserved electrostatic and structural motifs. *Protein Eng.* **11**, 415-420.

Bytyqi, A. H., Lockridge, O., Duysen, E., Wang, Y., Wolfrum, U. and Layer, P. G. (2004). Impaired formation of the inner retina in an AChE knockout mouse results in degeneration of all photoreceptors. *Eur. J. Neurosci.* **20**, 2953-2962.

Carmichael, S. L., Yang, W., Roberts, E., Kegley, S. E., Padula, A. M., English, P. B., Lammer, E. J. and Shaw, G. M. (2014). Residential agricultural pesticide exposures and risk of selected congenital heart defects among offspring in the San Joaquin Valley of California. *Environ. Res.* **135**, 133-138.

Carmichael, S. L., Yang, W., Roberts, E., Kegley, S. E., Brown, T. J., English, P. B., Lammer, E. J. and Shaw, G. M. (2016). Residential agricultural pesticide exposures and risks of selected birth defects among offspring in the San Joaquin Valley of California. *Birth Defects Res. A Clin. Mol. Teratol.* **106**, 27-35.

Cervantes, S., Yamaguchi, T. P. and Hebrok, M. (2009). Wnt5a is essential for intestinal elongation in mice. *Dev. Biol.* **326**, 285-294.

Chalmers, A. D. and Slack, J. M. W. (1998). Development of the gut in *Xenopus laevis*. *Dev. Dyn.* **212**, 509-521.

Chalmers, A. D. and Slack, J. M. (2000). The Xenopus tadpole gut: fate maps and morphogenetic movements. *Development* **127**, 381-392.

Cousin, X., Strahle, U. and Chatonnet, A. (2005). Are there non-catalytic functions of acetylcholinesterases? Lessons from mutant animal models. *BioEssays* **27**, 189-200.

Darboux, I., Barthalay, Y., Piovant, M. and Hipeau-Jacquotte, R. (1996). The structure-function relationships in Drosophila neurotactin show that cholinesterasic domains may have adhesive properties. *EMBO J.* **15**, 4835-4843.

Davidson, L. A., Marsden, M., Keller, R. and Desimone, D. W. (2006). Integrin alpha5beta1 and fibronectin regulate polarized cell protrusions required for Xenopus convergence and extension. *Curr. Biol.* **16**, 833-844.

de Almeida, P. G., Pinheiro, G. G., Nunes, A. M., Goncalves, A. B. and Thorsteinsdottir, S. (2016). Fibronectin assembly during early embryo development: a versatile communication system between cells and tissues. *Dev. Dyn.* **245**, 520-535.

Downes, G. B. and Granato, M. (2004). Acetylcholinesterase function is dispensable for sensory neurite growth but is critical for neuromuscular synapse stability. *Dev. Biol.* **270**, 232-245.

Drews, U. (1975). Cholinesterase in embryonic development. *Prog. Histochem. Cytochem.* **7**, V-VII, 1-49.

Dupree, J. L. and Bigbee, J. W. (1994). Retardation of neuritic outgrowth and cytoskeletal changes accompany acetylcholinesterase inhibitor treatment in cultured rat dorsal root ganglion neurons. *J. Neurosci. Res.* **39**, 567-575.

Dush, M. K. and Nascone-Yoder, N. M. (2013). Jun N-terminal kinase maintains tissue integrity during cell rearrangement in the gut. *Development* **140**, 1457-1466.

Duysen, E. G., Stribley, J. A., Fry, D. L., Hinrichs, S. H. and Lockridge, O. (2002). Rescue of the acetylcholinesterase knockout mouse by feeding a liquid diet; phenotype of the adult acetylcholinesterase deficient mouse. *Brain Res. Dev. Brain Res.* **137**, 43-54.

Ellman, G. L., Courtney, K. D., Andres, V., Jr. and Feather-Stone, R. M. (1961). A new and rapid colorimetric determination of acetylcholinesterase activity. *Biochem. Pharmacol.* **7**, 88-95.

Gilbert, M. M. and Auld, V. J. (2005). Evolution of clams (cholinesterase-like adhesion molecules): structure and function during development. *Front. Biosci.* **10**, 2177-2192.

Grisaru, D., Lev-Lehman, E., Shapira, M., Chaikin, E., Lessing, J. B., Eldor, A., Eckstein, F. and Soreq, H. (1999). Human osteogenesis involves differentiation-dependent increases in the morphogenically active 3' alternative splicing variant of acetylcholinesterase. *Mol. Cell. Biol.* **19**, 788-795.

Guo, X., Zhang, T., Hu, Z., Zhang, Y., Shi, Z., Wang, Q., Cui, Y., Wang, F., Zhao, H. and Chen, Y. (2014). Efficient RNA/Cas9-mediated genome editing in *Xenopus tropicalis*. *Development* **141**, 707-714.

Inkson, C. A., Brabbs, A. C., Grewal, T. S., Skerry, T. M. and Genever, P. G. (2004). Characterization of acetylcholinesterase expression and secretion during osteoblast differentiation. *Bone* **35**, 819-827.

Johnson, G. and Moore, S. W. (1999). The adhesion function on acetylcholinesterase is located at the peripheral anionic site. *Biochem. Biophys. Res. Commun.* **258**, 758-762.

Johnson, G. and Moore, S. W. (2004). Identification of a structural site on acetylcholinesterase that promotes neurite outgrowth and binds laminin-1 and collagen IV. *Biochem. Biophys. Res. Commun.* **319**, 448-455.

Johnson, G., Swart, C. and Moore, S. W. (2008a). Interaction of acetylcholinesterase with the G4 domain of the laminin alpha1-chain. *Biochem. J.* **411**, 507-514.

Johnson, G., Swart, C. and Moore, S. W. (2008b). Non-enzymatic developmental functions of acetylcholinesterase–the question of redundancy. *FEBS J.* **275**, 5129-5138.

Kedinger, M., Lefebvre, O., Duluc, I., Freund, J. N. and Simon-Assmann, P. (1998). Cellular and molecular partners involved in gut morphogenesis and differentiation. *Philos. Trans. R. Soc. Lond. B Biol. Sci.* **353**, 847-856.

Keller, M., Robitzki, A. and Layer, P. G. (2001). Heterologous expression of acetylcholinesterase affects proliferation and glial cytoskeleton of adherent chicken retinal cells. *Cell Tissue Res.* **306**, 187-198.

Layer, P. G., Weikert, T. and Alber, R. (1993). Cholinesterases regulate neurite growth of chick nerve cells in vitro by means of a non-enzymatic mechanism. *Cell Tissue Res.* **273**, 219-226.

Marsden, M. and DeSimone, D. W. (2001). Regulation of cell polarity, radial intercalation and epiboly in Xenopus: novel roles for integrin and fibronectin. *Development* **128**, 3635-3647.

Marsden, M. and DeSimone, D. W. (2003). Integrin-ECM interactions regulate cadherin-dependent cell adhesion and are required for convergent extension in Xenopus. *Curr. Biol.* **13**, 1182-1191.

Matsuyama, M., Aizawa, S. and Shimono, A. (2009). Sfrp controls apicobasal polarity and oriented cell division in developing gut epithelium. *PLoS Genet.* **5**, e1000427.

Mileson, B. E., Chambers, J. E., Chen, W. L., Dettbarn, W., Ehrich, M., Eldefrawi, A. T., Gaylor, D. W., Hamernik, K., Hodgson, E., Karczmar, A. G. et al. (1998). Common mechanism of toxicity: a case study of organophosphorus pesticides. *Toxicol. Sci.* **41**, 8-20.

Nieuwkoop, P. and Faber, J. (1994). *Normal Table of Xenopus laevis (Daudin)*. New York, NY: Garland Publishing.

Ohta, K., Takahashi, C. and Tosuji, H. (2009). Inhibition of spicule elongation in sea urchin embryos by the acetylcholinesterase inhibitor eserine. *Comp. Biochem. Physiol. B Biochem. Mol. Biol.* **153**, 310-316.

Pamanji, R., Bethu, M. S., Yashwanth, B., Leelavathi, S. and Venkateswara Rao, J. (2015a). Developmental toxic effects of monocrotophos, an organophosphorous pesticide, on zebrafish (*Danio rerio*) embryos. *Environ. Sci. Pollut. Res. Int.* **22**, 7744-7753.

Pamanji, R., Yashwanth, B., Bethu, M. S., Leelavathi, S., Ravinder, K. and Venkateswara Rao, J. (2015b). Toxicity effects of profenofos on embryonic and larval development of zebrafish (*Danio rerio*). *Environ. Toxicol. Pharmacol.* **39**, 887-897.

Paraoanu, L. E. and Layer, P. G. (2004). Mouse acetylcholinesterase interacts in yeast with the extracellular matrix component laminin-1beta. *FEBS Lett.* **576**, 161-164.

Pope, C., Karanth, S. and Liu, J. (2005). Pharmacology and toxicology of cholinesterase inhibitors: uses and misuses of a common mechanism of action. *Environ. Toxicol. Pharmacol.* **19**, 433-446.

Reed, R. A., Womble, M. A., Dush, M. K., Tull, R. R., Bloom, S. K., Morckel, A. R., Devlin, E. W. and Nascone-Yoder, N. M. (2009). Morphogenesis of the primitive gut tube is generated by Rho/ROCK/myosin II-mediated endoderm rearrangements. *Dev. Dyn.* **238**, 3111-3125.

Romero, P., Barnett, P. G. and Midtling, J. E. (1989). Congenital anomalies associated with maternal exposure to oxydemeton-methyl. *Environ. Res.* **50**, 256-261.

Sharma, K. V., Koenigsberger, C., Brimijoin, S. and Bigbee, J. W. (2001). Direct evidence for an adhesive function in the noncholinergic role of acetylcholinesterase in neurite outgrowth. *J. Neurosci. Res.* **63**, 165-175.

Sherman, J. D. (1995). Chlorpyrifos (Dursban)-associated birth defects: a proposed syndrome, report of four cases, and discussion of the toxicology. *IJOMEH* **4**, 417-431.

Silman, I. and Sussman, J. L. (2005). Acetylcholinesterase: 'classical' and 'non-classical' functions and pharmacology. *Curr. Opin. Pharmacol.* **5**, 293-302.

Sive, H. L., Grainger, R. M. and Harland, R. M. (2000). *Early Development of Xenopus laevis: A Laboratory Manual*. Cold Spring Harbor, NY: Cold Spring Harbor Laboratory Press.

Snawder, J. E. and Chambers, J. E. (1989). Toxic and developmental effects of organophosphorus insecticides in embryos of the South African clawed frog. *J. Environ. Sci. Health B* **24**, 205-218.

Soreq, H. and Seidman, S. (2001). Acetylcholinesterase - new roles for an old actor. *Nature Rev. Neurosci.* **2**, 294-302.

Spieker, J., Ackermann, A., Salfelder, A., Vogel-Höpker, A. and Layer, P. G. (2016). Acetylcholinesterase regulates skeletal in ovo development of chicken limbs by ACh-dependent and -independent mechanisms. *PLoS ONE* **11**, e0161675.

Spieker, J., Mudersbach, T., Vogel-Hopker, A. and Layer, P. G. (2017). Endochondral ossification is accelerated in cholinesterase-deficient mice and in avian mesenchymal micromass cultures. *PLoS ONE* **12**, e0170252.

Syed, M., Fenoglio-Preiser, C., Skau, K. A. and Weber, G. F. (2008). Acetylcholinesterase supports anchorage independence in colon cancer. *Clin. Exp. Metastasis* **25**, 787-798.

Trinh, L. A. and Stainier, D. Y. R. (2004). Fibronectin regulates epithelial organization during myocardial migration in zebrafish. *Dev. Cell* **6**, 371-382.

Vogel-Hopker, A., Sperling, L. E. and Layer, P. G. (2012). Co-opting functions of cholinesterases in neural, limb and stem cell development. *Protein Pept. Lett.* **19**, 155-164.

Weber, G. F., Bjerke, M. A. and DeSimone, D. W. (2012). A mechanoresponsive cadherin-keratin complex directs polarized protrusive behavior and collective cell migration. *Dev. Cell* **22**, 104-115.

Wyttenbach, C. R. and Thompson, S. C. (1985). The effects of the organophosphate insecticide malathion on very young chick embryos: malformations detected by histological examination. *Am. J. Anat.* **174**, 187-202.

Xiang, A. C., Xie, J. and Zhang, X. J. (2008). Acetylcholinesterase in intestinal cell differentiation involves G2/M cell cycle arrest. *Cell. Mol. Life Sci.* **65**, 1768-1779.

Xie, W., Stribley, J. A., Chatonnet, A., Wilder, P. J., Rizzino, A., McComb, R. D., Taylor, P., Hinrichs, S. H. and Lockridge, O. (2000). Postnatal developmental delay and supersensitivity to organophosphate in gene-targeted mice lacking acetylcholinesterase. *J. Pharmacol. Exp. Ther.* **293**, 896-902.

Yang, L., He, H.-Y. and Zhang, X.-J. (2002). Increased expression of intranuclear AChE involved in apoptosis of SK-N-SH cells. *Neurosci. Res.* **42**, 261-268.

Yarnitzky, T. and Volk, T. (1995). Laminin is required for heart, somatic muscles, and gut development in the Drosophila embryo. *Dev. Biol.* **169**, 609-618.
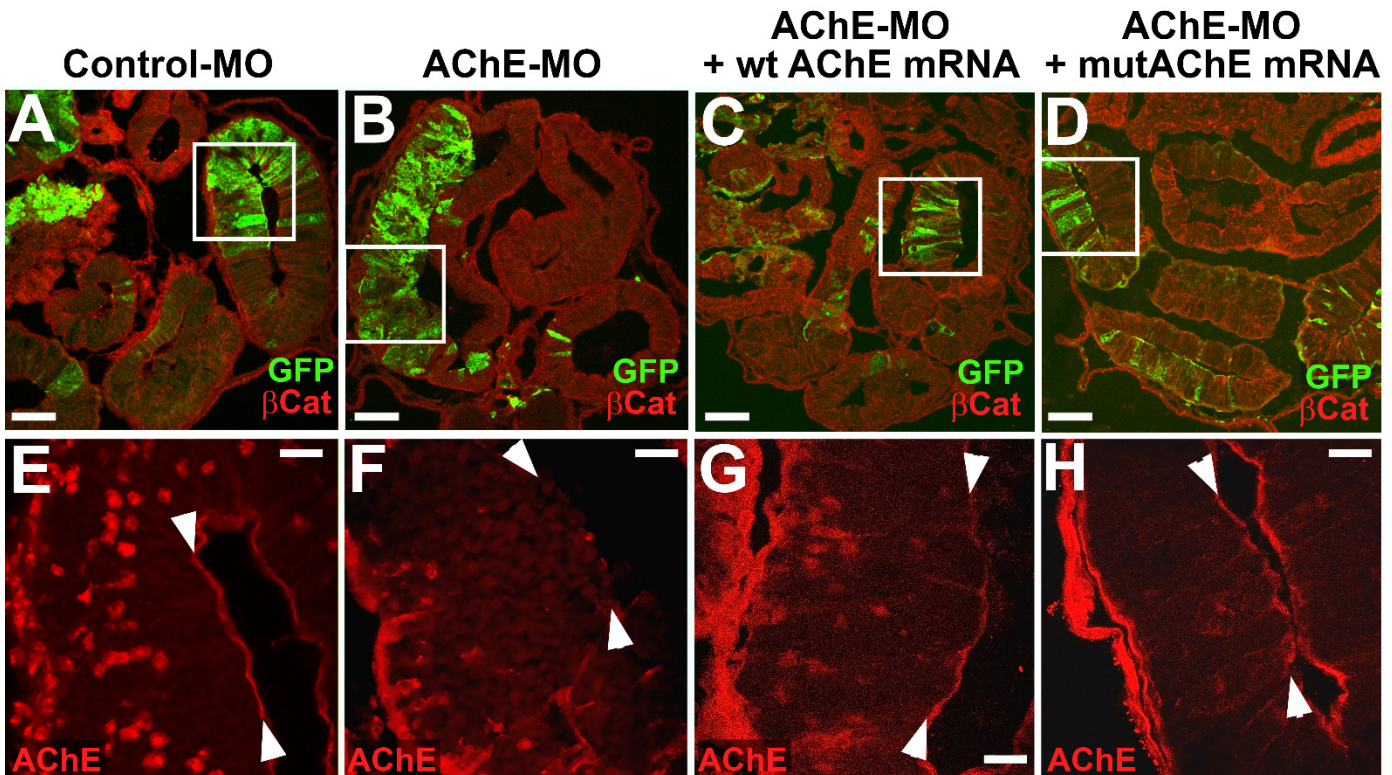
DEVELOPMENT

Figure S1) Morpholino-mediated knockdown of AChE protein expression. In sections through the intestine of NF 46 embryos injected with control MO (A), AChE MO (B), AChE MO + wt AChE mRNA (C), or AChE MO + mutAChE mRNA (D), β-catenin (red) outlines membranes of injected (i.e., GFP labeled; green) and un-injected cells. Serial sections from embryos in A-D were immunostained for AChE (red) and images of the boxed regions are shown at higher magnification (E-H). Apical localization of AChE protein (indicated by arrowheads in E-H) is observed in control MO injected cells (E), but is missing in AChE MO injected epithelium (F). AChE staining is rescued by co-injection with either wt AChE mRNA (G) or mutAChE mRNA (H). Scale bars = 100 μm (A-D); 25 μm (E-H).
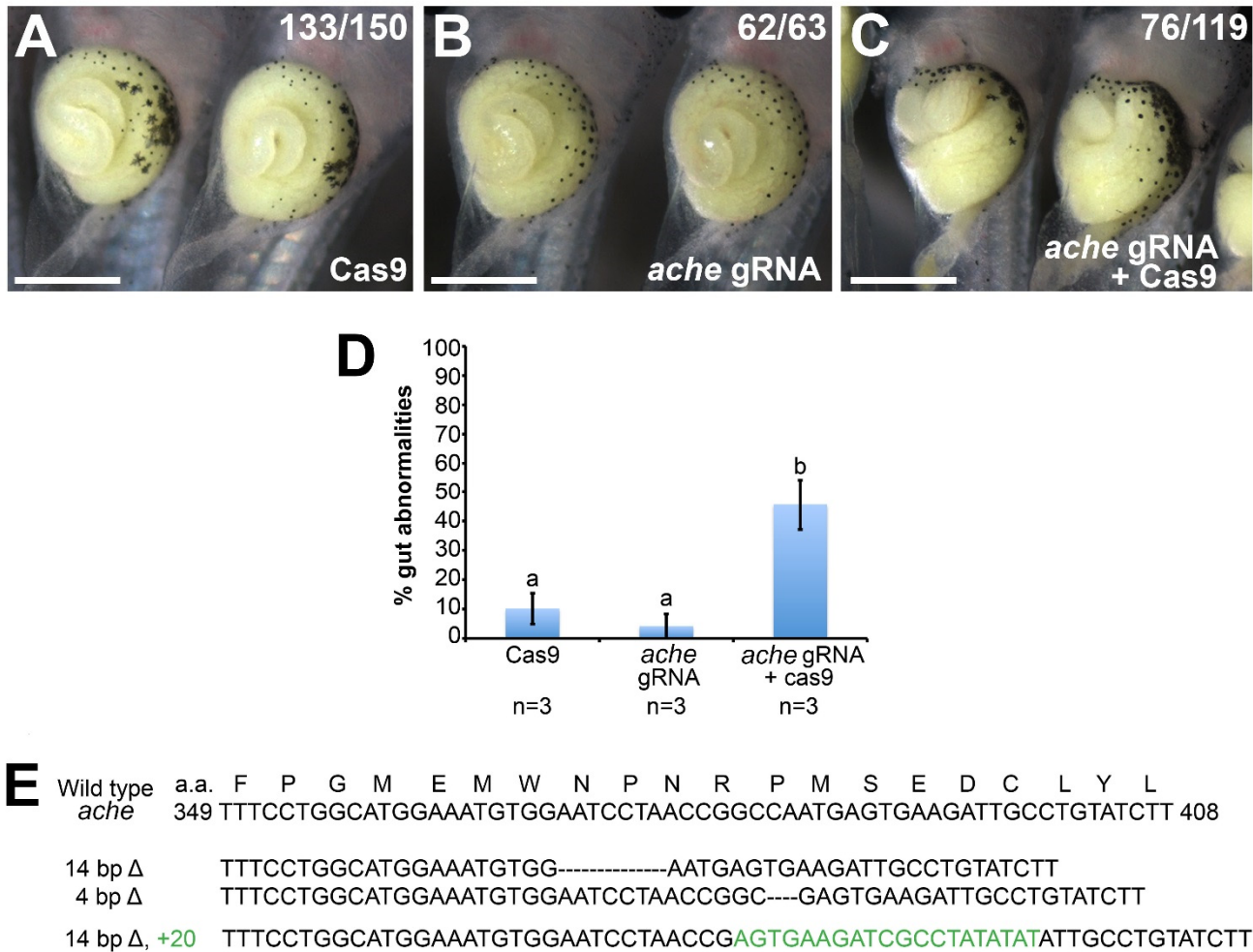
Figure S2) CRISPR-Cas9 mediated editing of *ache* gene perturbs gut elongation. *Xenopus* embryos were injected with Cas9 mRNA/protein (A), *ache* gRNA (B), or Cas9 plus *ache* gRNA (C), and allowed to develop until stage 46. Relative to injection of Cas9 or *ache* gRNA alone (A, B), injection of Cas9 plus *ache* gRNA (C) disrupts intestinal lengthening. Intestine phenotypes resulted from injection of Cas9 plus *ache* gRNA at both the 1- and 8-cell stages; craniofacial and spinal deformities, similar to those observed with AChE-inhibitor exposure, were also observed in embryos injected at the 1-cell stage (not shown), though absent in 8-cell endoderm targeted injections. The graph (D) indicates the mean (± S.E.M) percentage of embryos in which the intestine is shortened (n=3 different experiments, both 1- and 8-cell injections). E) Genomic sequencing validates the efficacy of CRISPR-Cas9 mediated editing, revealing the presence of deleterious mutations in representative Cas9 plus *ache* gRNA-injected embryos. Scale bars = 1000 μm.
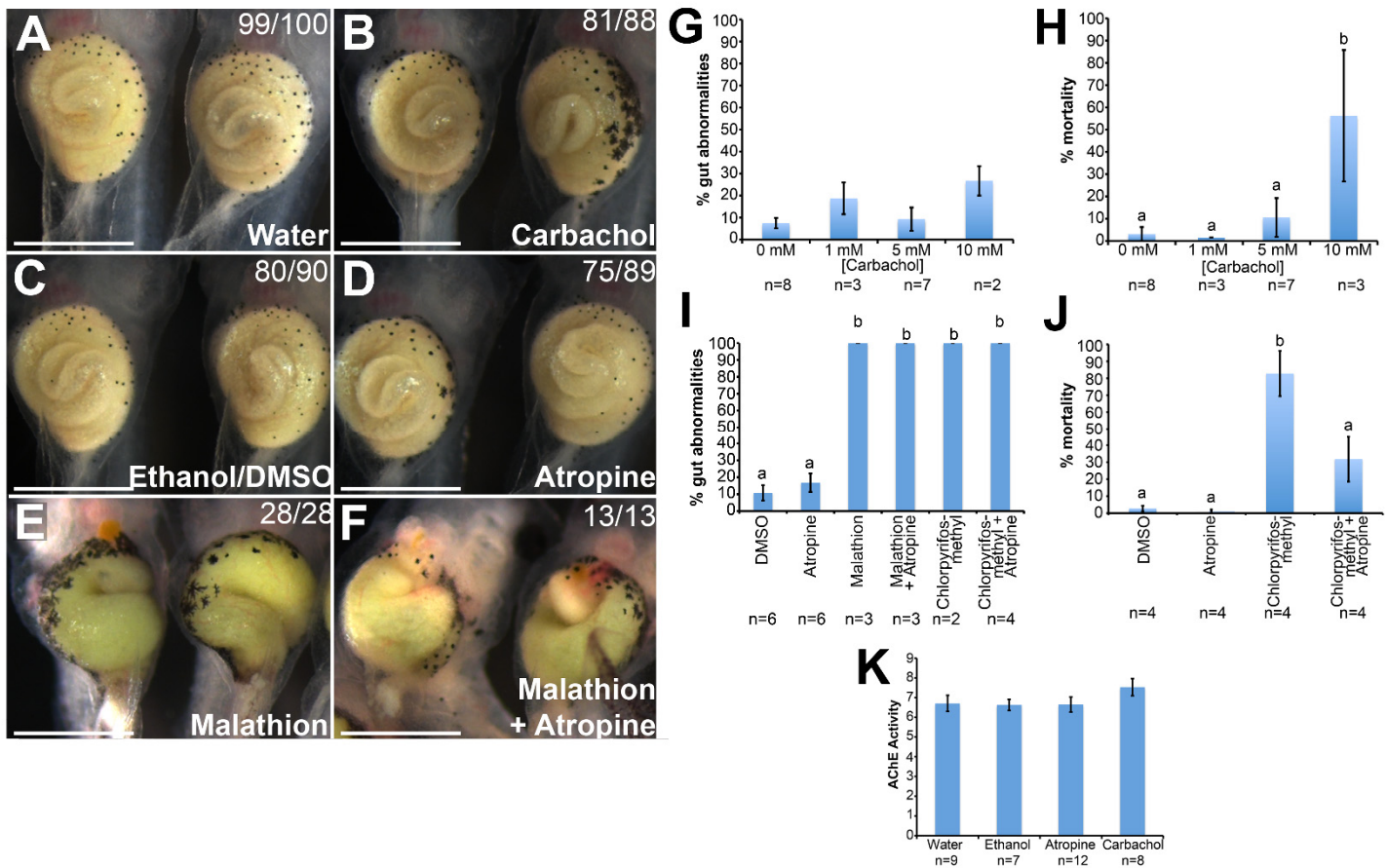
Figure S3) Modulation of cholinergic signaling via acetylcholine receptors (AChR) does not affect gut morphogenesis. Exposure of *X. laevis* tadpoles to the AChR agonist carbachol (B) from NF 33-46 does not affect elongation or rotation of the gut relative to water solvent controls (A). Similarly, exposure to the AChR antagonist atropine (D) has no impact on gut morphogenesis relative to DMSO/ethanol treated solvent controls (C). Gut elongation defects observed in AChE-inhibited embryos (e.g., Malathion; E) are not rescued by simultaneously blocking cholinergic signaling with atropine (F). Higher concentrations of carbachol do not affect intestinal development (G), but do result in a significant increase in embryonic lethality (H). Atropine does not rescue intestinal development in AChE inhibited embryos (I), but does reduce Chlorpyrifos-methyl (10mg/L) induced embryonic lethality (J). Neither atropine nor carbachol significantly alter AChE enzymatic activity (K). Scale bars = 1000 μm.
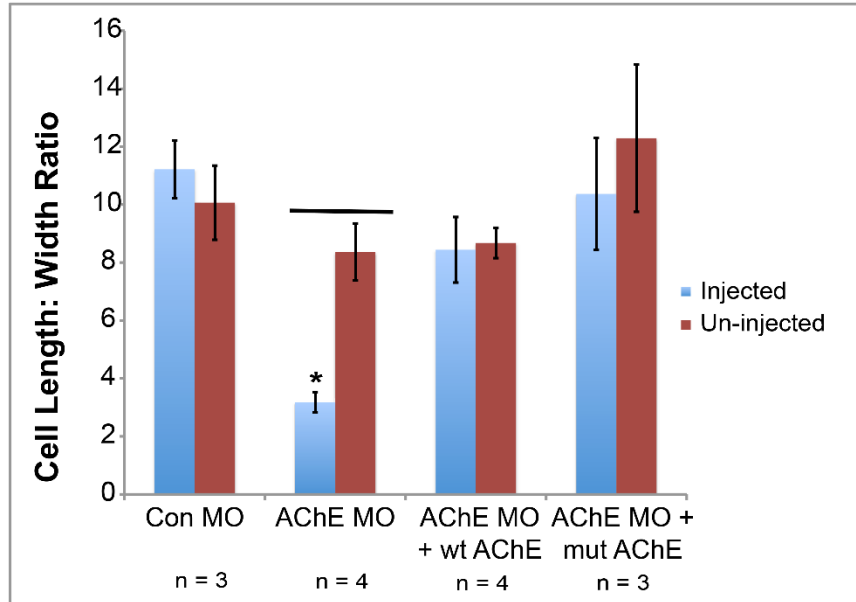
Figure S4) <u>Quantification of the effect of AChE on endoderm cell shape.</u> Length and width measurements were taken for at least 5 endoderm cells in each Control (Con) MO or AChE MO-injected embryo (+/- wt AChE or mutAChE mRNA) and the average L:W ratio calculated. Graphs represent mean L:W ratio for at least three embryos in each injection group ±S.E.M (n = number of individual embryos used to measure L:W ratios). Significant differences among injected cells are indicated by * (p<0.05). Significant differences between injected and un-injected cells within microinjection groups are indicated by a bar (p<0.05).
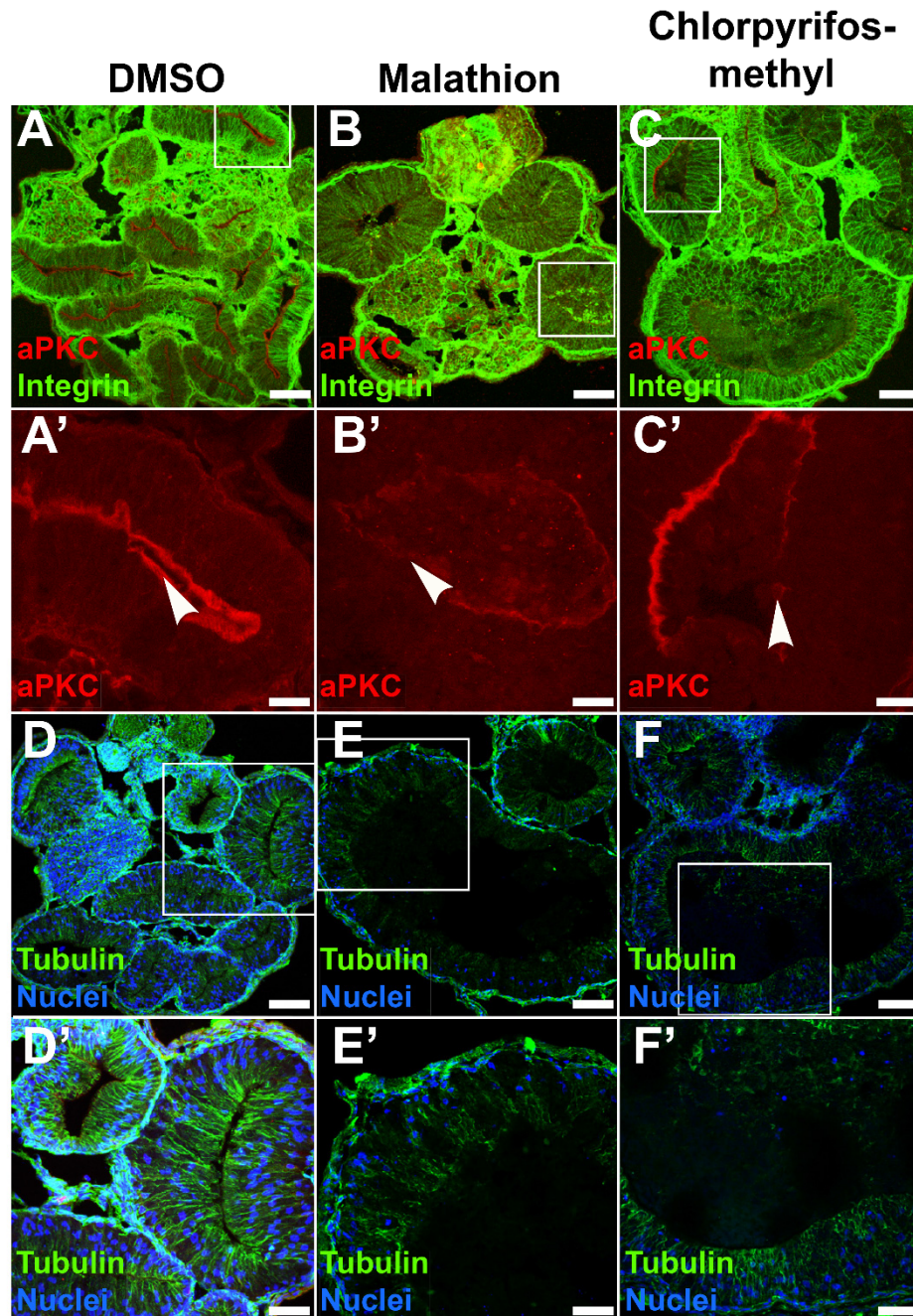
Figure S5) Chemical AChE inhibitors alter endoderm polarity, rearrangement and microtubule architecture. Transverse cross-sections through the gut of NF 46 tadpoles exposed to DMSO (A, A', D, D'), Malathion (B, B', E, E'), or Chlorpyrifos-methyl (C, C', F, F') from NF 33-46 were stained with integrin (A-C; green) to outline endoderm cell membranes, aPKC (A-C'; red) to highlight the apical surface of the epithelium, and alpha-tubulin (D-F'; green) to visualize microtubules. Compared with the columnar epithelium in DMSO exposed controls (A), the organization is disrupted in AChE inhibitor treated embryos (B, C). Arrowheads highlight robust apical expression of aPKC in DMSO controls (A'), versus patchy aPKC expression in chemically inhibited embryos (B', C'). Likewise, in DMSO controls (D, D'), α-tubulin bundles (green) are normally aligned along the apicobasal axis of the endoderm cells, with slight apical enrichment (D,D'); however, exposure to Malathion (E,E') or Chlorpyrifos-methyl (F,F') disrupts this architecture. Higher magnification images of the boxed regions in A-F are shown in A'-F'. Scale bars in A-C, D-F= 100 μm. Scale bars in D'-F'= 50 μm. Scale bars in A'-C' = 25 μm.
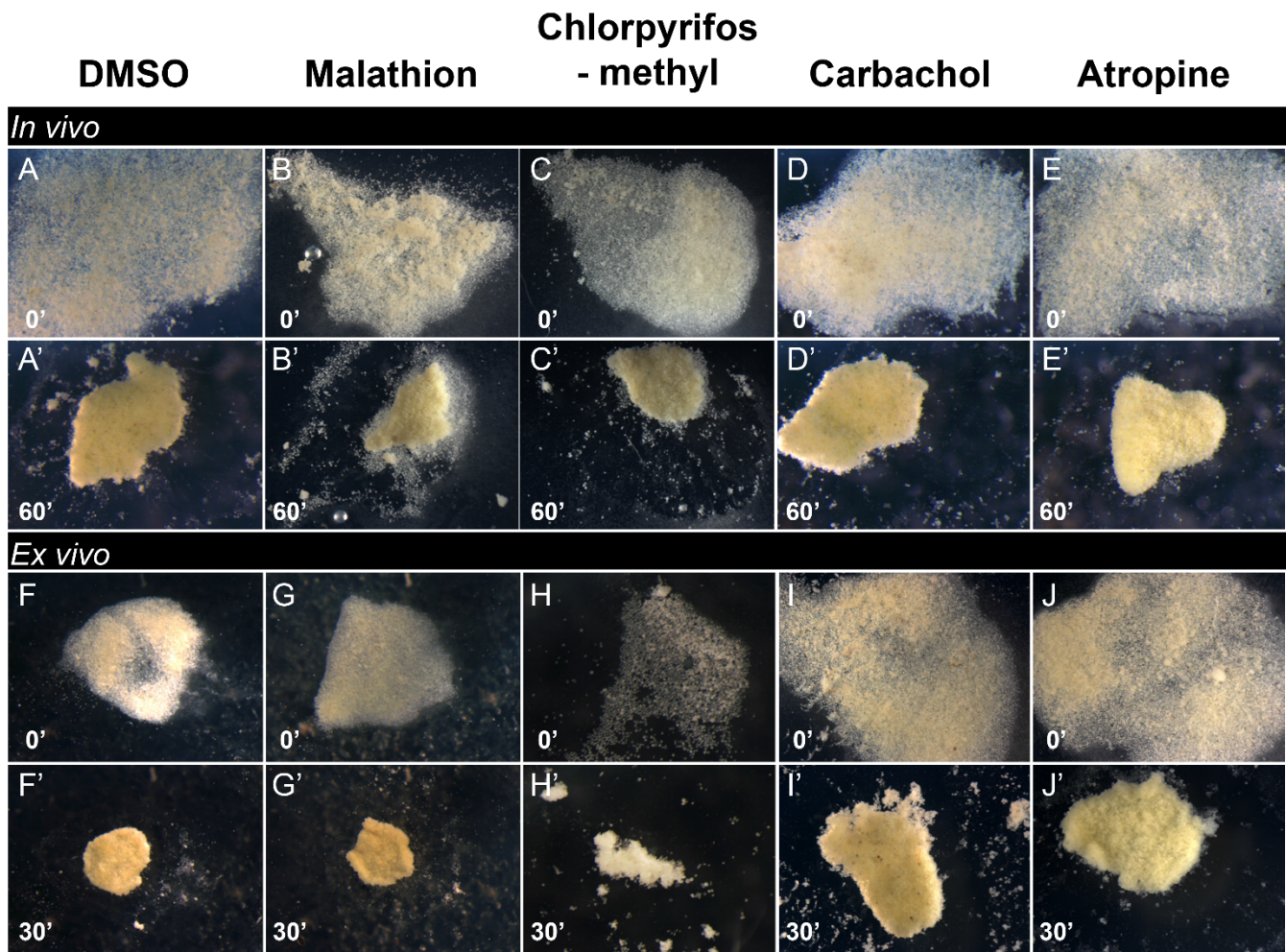
Figure S6) AChE activity is not required for endoderm cell-cell adhesion.
A-E') Endoderm cells were dissociated from four NF 41 tadpoles (A-E) previously exposed *in vivo* from NF 33-41 to DMSO (A,A'), Malathion (B,B'), Chlorpyrifos-methyl (C,C'), Carbachol (D,D') or Atropine (E,E'). Dissociated cells were allowed to re-aggregate for 60 minutes (60') after reintroduction of Ca^{2+} ions into the media (0'). Organophosphate inhibition of AChE (B-C'), chemical stimulation of cholinergic receptors (D,D'), or antagonism of cholinergic receptors (E,E') had no effect on re-aggregation (A'-E'), indicating cell-cell adhesion is independent of AChE or cholinergic signaling. At least three separate assays were performed per chemical.
F-J') Endoderm cells were dissociated (F-J) from four NF 41 tadpoles and subsequently exposed *ex vivo* to DMSO (F,F'), Malathion (G,G'), Chlorpyrifos-methyl (H,H'), Carbachol (I,I'), or Atropine (J,J') during a 60 minute re-aggregation assay. Organophosphate inhibition of AChE (G-H'), chemical stimulation of cholinergic receptors (I, I'), or antagonism of cholinergic receptors (J, J') had no effect on re-aggregation (F'-J'), indicating cell-cell adhesion is not mediated by AChE or cholinergic signaling.

Supplemental Materials and Methods

Chemical exposures

Xenopus laevis tadpoles were exposed to a range of AChE inhibitor concentrations (1-50 mg/L malathion, 1-10 mg/L chlorpyrifos-methyl, or 0.1-15 µM Huperzine A) or to an equivalent volume of DMSO solvent from NF 33-46 to identify doses that consistently disrupted intestinal development but were not overtly lethal.

mRNA generation and synthesis

A pCS2 vector containing a coding region for cMyc tagged GFP was linearized with *Not1*, capped mRNA synthesized with the mMessage Machine kit (Ambion), and purified by lithium chloride extraction. Total RNA was isolated from ten NF 41 tadpole intestines using TRIzol (Ambion) and RT-PCR (Superscript) used to generate cDNA. *Xenopus laevis* AChE was amplified with Pfu Ultra II polymerase (Agilent) using the following forward and reverse primers:

F: 5' GCCGGATTCATGGCACTTGTACCC 3'
R: 5' ATGTGGAACCCCCATCCACTGTGGCCAAG 3'

These primers incorporate new restriction sites upstream of the transcription start site, creating a new MO-resistant 5' UTR for subsequent wt and mutAChE synthesis.

Wt AChE DNA was inserted into the pCS2 vector and transformed into competent *E. coli* cells. The conserved serine (Ser224 in *X. laevis*) in the esterase catalytic triad was mutated to an alanine with PCR using the following forward and reverse primers:

F: 5' GGGGAAGCTGCTGGTGCCGTCTCTGTGGG 3'
R: 5' ACCAGCAGCTTCCCCAAAAATCATGACAGTCCTGGGATC 3'

The resultant mutAChE product was inserted into the pCS2 vector (NEBuilder HiFi DNA assembly kit) and mutation confirmed by sequencing. Wt and mutAChE mRNA was synthesized as described for GFP.

AChE Activity Assays

Stage 46 embryos from chemical exposure and Stage 35 embryos from 1-cell MO and AChE mRNA microinjections were anesthetized in 0.05% MS222 and frozen at -80°C in groups of four. Embryos were homogenized in 1% Triton 0.05M Tris-HCL (pH 7.4) buffer at a 1:10 (w:v) ratio and centrifuged for 5 minutes at 15,000 x g at room temperature. Protein concentrations were determined with the Pierce BCA protein assay (ThermoScientific). Protein preparations were used in the Ellman AChE activity assay, modified for use in a 96 well plate (Ellman et al., 1961). Briefly, 20 µg of protein was added to 1% Triton 0.05 M Tris-HCL (pH 7.4) buffer (total volume = 300 µL). 10 µL of 0.33mM f,f'-dithio-bis (2-nitrobenzoic acid) (DTNB) was added per well and the plate incubated at room temperature for 10 minutes. 2 µL of 0.075 M acetylthiocholine iodide was added per well and the absorbance read at 412 nm for 15 minutes. All samples were read in triplicate and 300 µL Tris buffer with DTNB and acetylthiocholine iodide served as a blank. Activity was calculated as nmol acetylthiocholine iodide hydrolyzed per minute per µg protein.

Immunohistochemistry

Table S1. Primary antibodies, antibody suppliers, and concentrations used for indirect immunofluorescence.

Antibody	Supplier	Concentration
E-cadherin	DSHB 5D3	1:200
β1-Integrin	DSHB 8C8-c	1:1000
β-catenin	SCBT H-102	1:100
aPKC	Santa Cruz sc216	1:200
α-tubulin	Sigma T9026	1:1000
Active caspase 3	Cell Signaling Technology 9661	1:300
cMyc	Santa Cruz 9E10	1:1000
AChE	Abcam ab 97298	1:200
GFP	ThermoFisher A6455	1:500
pH3	Millipore 06-570	1:500
IFABP	Gift from Yun-Bo Shi	1:1000
Fibronectin	Gift from D.W. DeSimone	1:1000
Laminin	Sigma L9393	1:200
Alexa 488 – conjugated goat anti-mouse IgG	ThermoFisher A11029	1:2000
Alexa 488 – conjugated goat anti-rabbit IgG	ThermoFisher A11034	1:2000
Alexa 546-conjugated goat anti-rabbit IgG	ThermoFisher A11035	1:2000
Alexa 546-conjugated donkey anti-mouse	ThermoFisher A31570	1:2000

Ex vivo Cell Adhesion Assays

Whole guts were dissected from untreated, chemically-treated or MO-injected NF 41-42 tadpoles. Foreguts were discarded and the primitive intestine splayed open along the anterior-posterior axis and everted so that the endoderm cells faced the media. Intestine explants were transferred to 9 mL calcium magnesium free media (CMFM) in a 1% agarose-coated well of a 12-well plate, and allowed to dissociate for 30 minutes at room temperature (Sive et al., 2000). Eyelash knives were used to further separate endoderm cells from the gut tube, and the underlying mesoderm was discarded.

Dissociated endoderm cells were used to assess both cell-cell and cell-substrate adhesion. For cell-cell adhesion assays, dissociated cells were left in 1% agarose-coated dishes. Most of the CMFM was drawn off and the media replaced with 1X MBS containing calcium and magnesium ions. Cells were allowed to re-aggregate for 30-60 minutes at RT.

For cell-substrate adhesion assays, individual wells of a 12-well plate (or the equivalent surface area of a 60 mm plastic petri dish) were coated with 50 μg/ml laminin (Sigma L2020) at 4°C overnight, washed with sterile PBS, and blocked with 0.2% BSA for 1 hour at 37°C. Wells were washed with 1X PBS and 4 mL of cell media added (50% 1X MBS, 49% Leibovitz solution, 1% FBS, 50 μg/mL Gentamycin) (Sternfeld et al., 1998). Alternatively, wells were coated with 50 μg/ml fibronectin (Sigma F1141) for 30 minutes at room temperature, rinsed three times with 1X PBS, and 4 mL of cell media added. Dissociated endoderm cells were transferred to either laminin- or FN-coated plates and five 12X images of each plate were taken with a Zeiss Lumar microscope to determine the initial number of plated cells. Cells were allowed to adhere for ~60 minutes at room temperature, when most of the cell media was removed from each plate and cells washed three times with 1X MBS. The remaining adherent cells were fixed in formaldehyde-glutaraldehyde (FG) overnight at 4°C. The FG was then removed and the plates washed three times with PBST. Five 12X images of each plate were acquired after fixation to determine the number of adherent cells on each substrate. Adobe Photoshop CS6 was used to automatically align the five images for each plate in order to merge the entire field of plated or adherent cells. FIJI was used to automatically threshold images and quantify cell number. The percentage of adherent cells on each plate was determined by dividing the number of adherent cells by the number of plated cells and multiplying by 100.